Infrared Spectroscopy of Water and Zundel cations in Helium Nanodroplets

Deepak Verma[1,*], Swetha Erukala[1] and Andrey F. Vilesov[1,2]

[1] Department of Chemistry, University of Southern California, Los Angeles, California 90089, USA
[2] Department of Physics and Astronomy, University of Southern California, Los Angeles, California 90089, USA

* Present address: Intel Corporation, RA3-K13, 2501 NE Century Blvd, Hillsboro, Oregon 97124, USA

Abstract

Here, we show that electron impact ionization of helium (He) droplets doped with water molecules and clusters, yield water and Zundel cations embedded in the droplets consisting of a few thousand helium atoms. Infrared spectra in the OH-stretching range were obtained using release of the cations from the droplets upon laser excitation. The spectra in He droplets appear to have about a factor of 10 narrower bands and similar matrix shifts as compared to those obtained via tagging with He and Ar atoms. The results confirm the calculated structure of the free Zundel ion, where the proton is equidistant from the two water units. The effect of the He environment on the spectra of ions is discussed. The signal shows nonlinear laser pulse energy dependence consistent with evaporation of the entire droplet upon multiple absorption of infrared photons. This conclusion is supported by the model calculations of the efficiency of the cations' release versus laser flux.

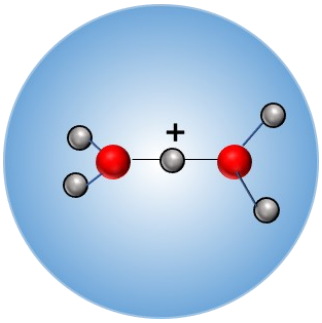

1. Introduction

Molecular ions are important intermediates in chemistry of condensed phase and upper atmosphere as well as in astrochemistry.[1-3] Infrared spectroscopy has been widely used for interrogation of the structure of ions as well as their reactivity and interaction with solvent species. Therefore, great strides were done in developing new techniques for spectroscopy of ions. Absorption spectra of small molecular cations such as H_2O^+ and H_3O^+ have been obtained in discharge experiments.[4, 5] In comparison, the study of larger molecular cations and ionic clusters involves action spectroscopy in molecular beams. Typically, the ions of interest are tagged with noble gas atoms or hydrogen molecules, while the absorption is tracked by dissociation of the complexes.[6-8] The tagging may cause some splitting of the bands of ionic complexes due to lowering of symmetry or the presence of isomers. Thus, the interpretation of the spectra may require extensive quantum chemical calculations. Recently introduced cooling in cryogenic traps filled with He gas has enabled lowering the temperature of the cations to ~ 5-10 K and tagging with most weakly bound He atoms.[9-11] Experiments in cryogenic traps were also used to attain the spectra of free (untagged) ions such as CH_5^+ [12] by monitoring faster reactivity of vibrationally excited ions.

Isolation in solid matrices presents another successful approach to spectroscopy of ions, [13, 14] which does not however, offer a mass spectrometric identification required for study of ionic clusters. The low temperature (~ 0.4 K), liquid state, weak interaction, and high ionization potential of helium (He) atoms makes helium droplets an ideal matrix for spectroscopy of ions. He droplet spectroscopy has been extensively applied for neutral species and relies on depletion of the He droplet beam upon infrared absorption of the embedded species.[15-19] The depletion technique could not be applied to the embedded ions due to very low fraction of droplets containing ions. Observation of the ejection of molecular ions from the droplets upon infrared irradiation by M. Drabbels *et. al.*[20] has prompted further advances in the field. In the first experiments, the embedded aniline ions were produced through resonance-enhanced multiphoton ionization of the embedded molecules.[20] Alternatively, G. von Helden and co-workers produced ions through electrospray, stored them in an ion trap followed by pickup by the droplet.[21] Employing photoionization and electrospray techniques require more involved apparatus as compared to He droplet depletion spectroscopic experiment and also imposes limitations on the kind of ions that could be produced.

Here, we turn our attention to electron impact ionization (EI) which is a reliable and a well-established technique. It is long known that EI of droplets containing few thousands of He atoms doped with neutral species leads to effective production of molecular ions and various ionic fragments.[22, 23] Ionization of embedded atoms, A, leads to formation of He_nA^+ clusters, with up to few tens of He atoms. However, the production of the He complexes with molecular ions is much less efficient, which likely relates to formation of vibrationally excited ions and concomitant dissociation of He atoms.[22, 23] Few noticeable exceptions include fullerenes, such as C_{60}, as studied in group of P. Scheier which was found to form a long progression of $He_nC_{60}^+$ containing up to about 100 attached He atoms.[24] Larger mass of C_{60} also helps in dramatically reducing interference from diverse small ions, such as He_n^+ and rest gas species. Laser induced dissociation of the $He_nC_{60}^+$ was used to study the solvation of C_{60}^+ with atomic resolution.[24] A. Ellis *et al.* recently produced complexes of protonated acetic acid tagged with one or two He atoms [25] and protonated carbon dioxide with up to 14 He atoms [26] upon EI of the doped He droplets containing about 5000 He atoms. The infrared spectra were obtained via depletion infrared laser spectroscopy of the complexes.

Spectroscopic study of ions through solvation in droplets of few thousand He atoms appears more favorable than through tagging by few atoms, since the droplets offer a homogeneous environment with a well-defined temperature of about 0.4 K [27] leading to narrower spectral lines. Our experimental approach rests on the conjecture that some unknown fraction of ions produced via EI of the doped droplets remain solvated in the droplets of a few thousand He atoms.

In this work, we show that through EI, ionic species embedded in the droplets can be formed, making it a convenient technique for producing a wide variety of embedded ions and ionic clusters. Infrared spectra are obtained by measuring the intensity of the cations released from the droplets upon laser excitation. Additionally, we report the OH-stretch spectra of water (H_2O^+) and Zundel ($H_5O_2^+$) cations in helium droplets in the 3 μm region. These important cations were chosen as candidates for validation of this newly developed technique. The spectra are compared with the earlier results obtained by tagging and followed by discussion on the structure of the ions and their interaction with the superfluid helium environment. The signal shows nonlinear laser pulse energy dependence consistent with evaporation of the entire droplet upon multiple absorption of infrared

photons. The results of the model calculations suggest a possible improvement in the performance of our technique upon moderation of the droplet sizes.

2. Experimental setup

This work builds on modifications to a molecular beam UHV vacuum apparatus, which has previously been used for spectroscopy of neutral species.[16-19] Figure 1 shows the schematics of the experimental apparatus. He droplets are produced upon expansion of helium gas at stagnation pressure of P_0 = 20 bars and temperature of T_0 = 23 K in vacuum through a 1 mm diameter pulsed nozzle (General Valve series 99) attached to a Sumitomo RDK 408 refrigerator.[28] The nozzle produces pulses of He droplets of about 100 - 200 μs width which is controlled by a pulse driver (IOTA ONE).[28, 29] Upon collimation by a 2 mm diameter skimmer, He droplets enter the pickup chamber where they capture water molecules. Going further downstream, the doped droplets enter the detection chamber that hosts a quadrupole mass spectrometer (QMS) (Extrel MAX 500) equipped with a standard axial electron impact ionizer, which will be referred to as probe ionizer. An additional axial ionizer (here referred as external ionizer), same as probe ionizer, is placed ~ 20 cm upstream from the QMS probe ionizer and has a stack of Einzel lenses for separation of light and heavy ions.

When the probe ionizer is ON and external ionizer is OFF, the set-up is equivalent to that as used for depletion spectroscopy of neutral species.[16] This mode is used for aligning of the He droplet beam, initial adjustment of the pickup pressure, and determination of the flight time of the droplets from the nozzle to the QMS. For spectroscopy of ions, the external ionizer is ON and typically set up to an electron energy of 100 eV and emission current of 10 mA. In this mode, the probe ionizer is OFF, while the ion optics voltages (ion range, extraction *etc*.) are ON and set to the same values as during the standard probe operation. Electron impact of the doped droplets in an external ionizer leads to a large variety of products, such as He_n^+, free splitter ions of the dopants, as well as dopant and splitter ions embedded in the droplets. The heavy droplets containing ions continue traversing towards the QMS, whereas the light ions produced post ionization are rejected by the Einzel lenses, which act as a high pass filter.

The doped ionic droplets are irradiated by a pulsed infrared laser beam when they pass through the ion range of the probe ionizer. The laser beam is set to counter propagate with the

droplet beam and is focused into the ion range of the probe by a 25 cm focal length lens. Absorption of several infrared quanta leads to production of free ions, which are then extracted, mass selected and detected by the QMS. Infrared spectra are recorded by monitoring the gated (~ 10 μs) QMS signal of the bare ions set at a desired mass (M =18 and 37 for H_2O^+ and $H_5O_2^+$, respectively), as the laser frequency is scanned. The spectra are obtained using a pulsed optical parametric oscillator-amplifier (Laser Vision, spectral resolution: ~ 0.1 cm^{-1}, pulse duration ~ 7 ns, pulse energy ~ 5 - 8 mJ, repetition rate 20 Hz). The absolute frequency of the laser is calibrated using the photo-acoustic spectrum of methane and ammonia molecules.

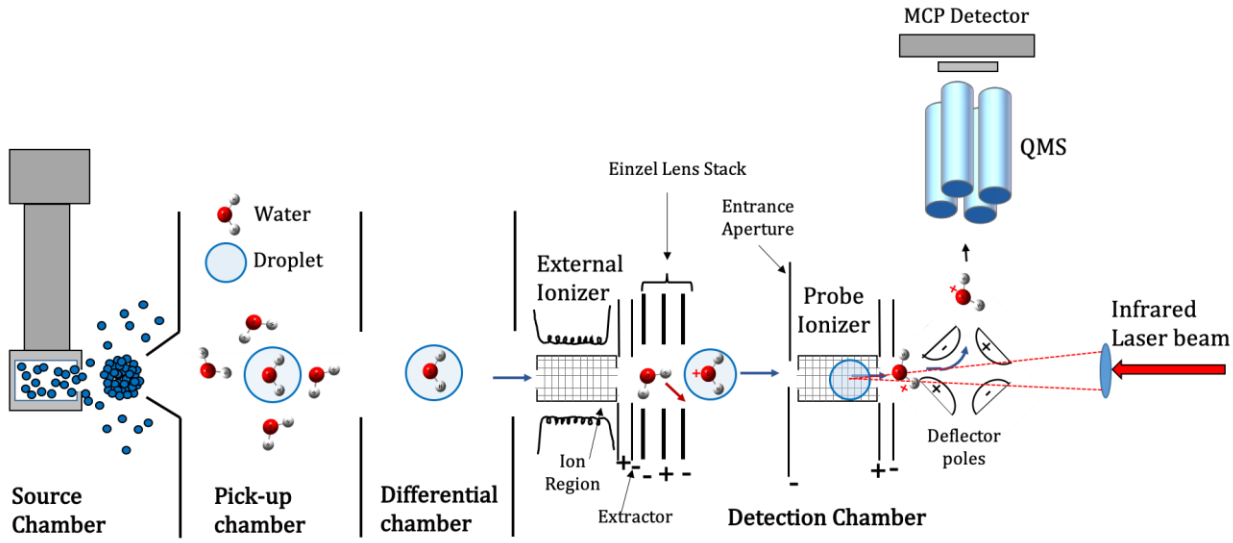

Figure 1. Schematic of helium droplet setup for molecular ion spectroscopy. He droplets are produced from a cold pulsed nozzle in the source chamber. The He droplets capture dopants in the pickup chamber and traverse into the detection chamber equipped with two electron impact ionizers: External and Probe. The droplets are ionized in the external ionizer and interact with the counter propagating infrared laser beam once in the ion region of the probe ionizer. The released ions are mass selected by the quadrupole mass spectrometer.

3. Results and Discussion

3.1. Water Ions

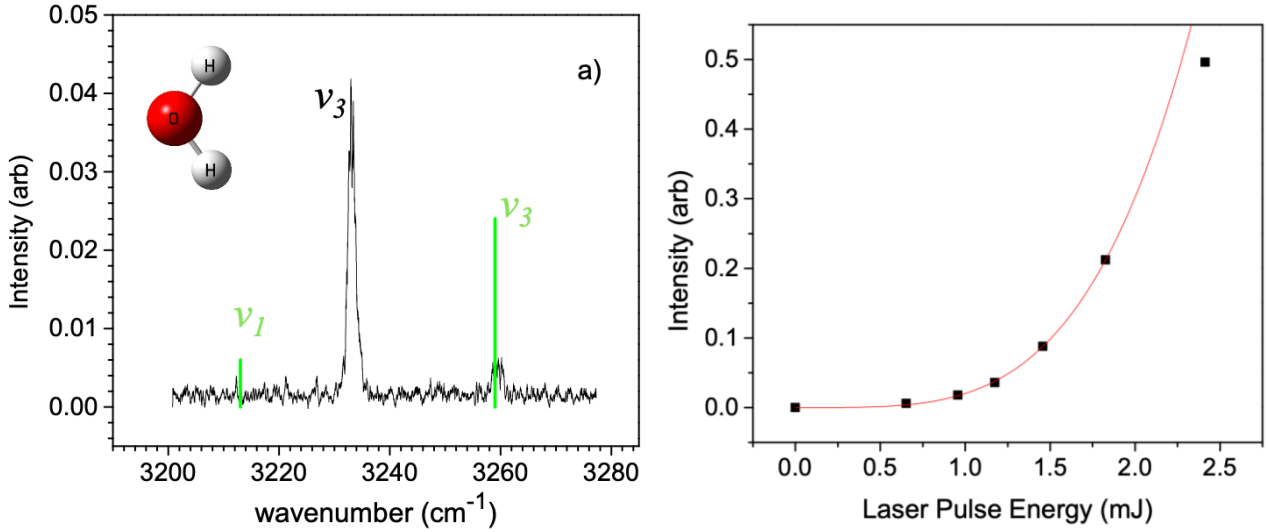

Figure 2. (a) Spectrum of H_2O^+ in helium droplet of ~ 7×10^3 atoms as measured at laser pulse energy of ~ 5 mJ/pulse. Measurement time is about 10 min. The origins of the ν_1 and ν_3 bands of the free ions are marked by green vertical bars, whose heights are proportional to the infrared intensity.[5] (b) Intensity dependence of ν_3 band versus the laser pulse energy (E): Black squares represent the experimental results while the red curve shows a fit by $I = a \cdot E^{3.9}$ for $E < 2$ mJ.

Figure 2 (a) shows the spectrum of water ions in He droplets. Water molecules were picked up upon admitting water vapor at 1×10^{-6} mbar into the pickup chamber, the pressure maximizing the laser induced ion signal. The average size of He droplets, $N_{He} \approx 7000$, is estimated through the Poisson pickup pressure dependence of the ion signal assuming that the pickup cross section equals to the average geometric cross section of the droplets. An intense peak at 3233.0 cm^{-1} is assigned to the asymmetric O-H stretch, ν_3. A second weaker peak is also seen at ~ 3259.6 cm^{-1}, whose assignment is less clear. In free H_2O^+ ions, the origins of the symmetric, ν_1 , and asymmetric, ν_3 , bands were found at 3213 cm^{-1} and 3259 cm^{-1}, respectively, which are shown by green bars in Figure 2 (a).[5] In earlier studies by Dopfer *et al.,* [30] ν_1 = 3198 cm^{-1} and ν_3 = 3254 cm^{-1} were found in He-H_2O^+ complexes. Larger shift of the $\Delta\nu_3$ = ~ 26 cm^{-1} in He droplets, with respect to free ions, is likely related to the cumulative effect of the liquid helium environment, where the first solvation shell of the ion is made of ~ 15 He atoms. We did not observe any significant peaks in the broader survey scans at frequency below 3200 cm^{-1}. However, there is a possibility that such a peak may have been missed due to low intensity owing to non-linear laser pulse energy of the signal as described in the following.

We have also considered the possibility where the 3259.6 cm^{-1} peak is assigned to the ν_1 band. Reversal of the ν_1 and ν_3 bands has been found in Ar_2-H_2O^+ complexes with Ar atoms bound to protons (H-bound).[8, 31, 32] According to calculations for He-H_2O^+ complexes,[30] He atoms are strongly bound to the protons (H-bound) (D_e = 520 cm^{-1}) whereas the binding is weaker for the *p*-bound (D_e = 230 cm^{-1}) and O-bound (D_e = 60 cm^{-1}). Therefore, it is feasible that the primary spectroscopic unit may be regarded as C_{2v} He_2-H_2O^+ complex having two H-bound He atoms. It is interesting to see that in Ar_4-H_2O^+ complexes the splitting between the ν_1 and ν_3 bands diminishes, which was assigned to the effect of the *p*-bonding of the additional Ar atoms.[8, 31] In Ne and Ar matrices, ν_1 was found at lower frequency than ν_3, same as in gas phase.[33, 34] Another possible assignment of the 3259.6 cm^{-1} peak is to a combination band of ν_3 and vibrations of He atoms.

It is known that the spectra of small molecules in helium show rotational structure.[16, 18, 19] In particular, water molecules in helium droplets have similar rotational constants as in free molecules.[35] The rotational constants of the free water ion are known to be A= 28.0 cm^{-1}, B = 12.4 cm^{-1} and C = 8.5 cm^{-1}.[5] The fact that no rotational structure was observed for water ions indicates a large reduction of the rotational constants in helium. Assuming, that the primary molecular unit of an ion concerning the ro-vibrational spectra is He_2-H_2O^+, with two He atoms in the H-bound

positions, the rotational constants could be estimated based on the structure of the He-H_2O^+ complexes[30] to be A = 1.31 cm^{-1}, B = 0.42 cm^{-1} and C = 0.32 cm^{-1} . The values of the rotational constants are expected to be significantly lower in He environment. This effect is well documented for neutrals where the rotational constants decrease by about a factor of three, depending on the particular molecule.[16-19] As a result, the rotational structure of the v_3 band in He could not be resolved in agreement with the experimental observations. The v_3 band in Fig. 2 (a) has a width (FWHM) of ~ 2 cm^{-1}. This is comparable to the width of ro-vibrational lines of water molecules in He in the range of 0.3 – 3 cm^{-1},[35] and the width of bands of larger molecules with unresolved rotational structure in He.[16, 18, 19] Therefore, a factor of ~ 10 stronger interaction of ions with the nearest neighbor He atoms as compared with neutrals, does not cause any excessive line broadening.

Figure 2 (b) shows the laser pulse energy (E), dependence of the intensity of the v_3 band in Fig. 2 (a). E was measured at the entrance window to the vacuum apparatus and varied by changing of the energy of the NdYAG pump. At the highest laser pulse energy of ~ 2.5 mJ, ~ 10 water ions were detected per each pulse. It is seen that the dependence is nonlinear, whereas at low pulse energy the intensity scales as $\sim E^4$. The nonlinear dependence of the intensity distorts the true infrared intensity ratio of the bands, making weaker bands even weaker. The mechanism of the ion release from the droplets upon laser irradiation and the E - dependence will be discussed in Section 3.3.

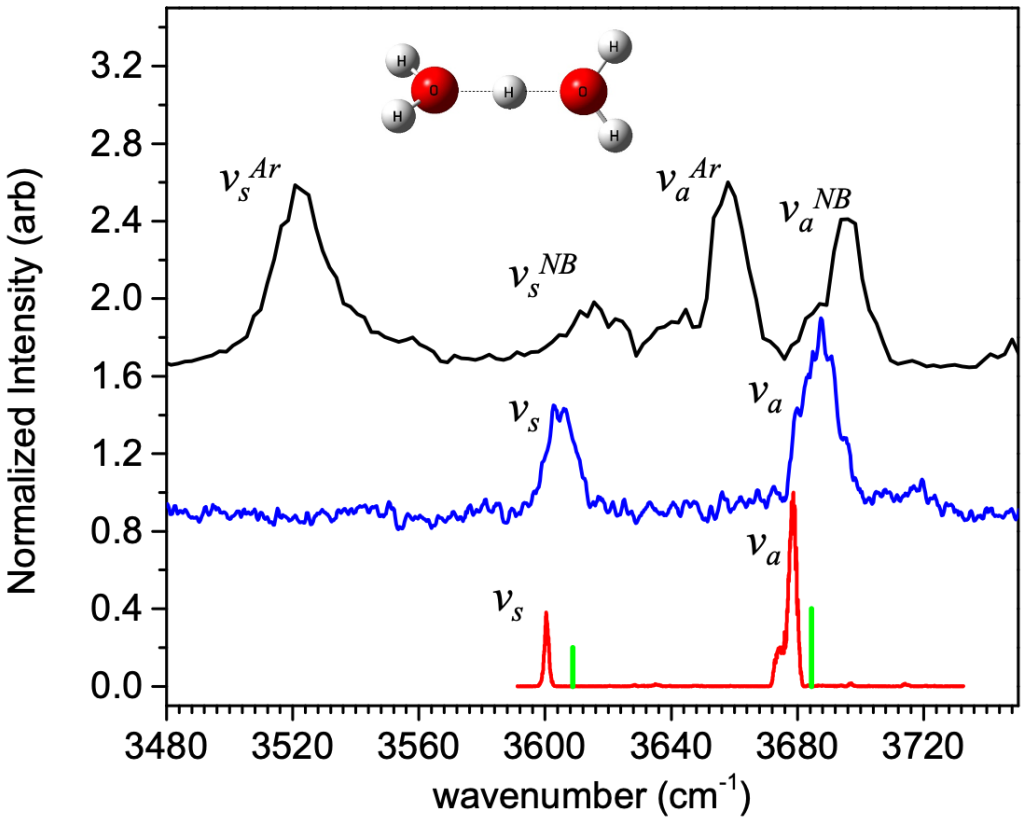

Figure 3. Spectrum of $H_5O_2^+$ in He droplets (red), compared with the spectra of He-$H_5O_2^+$ (blue) [10] and Ar-$H_5O_2^+$ (black).[36] The band origins of the free ions are marked by green vertical bars,[37] whose heights are proportional to the infrared intensity.[38]

3.2. Zundel Ions

Red trace in Figure 3 shows the spectrum of Zundel ion ($H_5O_2^+$), in helium droplets. The spectrum was measured upon the pickup of several water molecules in the pickup chamber filled with water vapor at 2×10^{-6} mbar. The trace represents a true zero background measurement, whereas some noise seen in Figure 2 (a) is due to a spurious background signal from water from the rest gas. According to previous computational studies,[38, 39] the proton in Zundel ion has a minimum potential energy configuration of C_2 symmetry and the proton equidistant from the two water moieties, which are staggered by about 100 degrees. Large amplitude motion of the H_2O moieties results in an effective D_{2d} symmetry of the complex.[38] The geometry of the H_2O-H^+ units is close to pyramidal. The $H_5O_2^+$ has two symmetric (ν_s) and two antisymmetric (ν_a) OH stretching modes.[37] Only the out of phase symmetric stretch has an appreciable infrared intensity. However, the in phase and out of phase antisymmetric stretches are predicted to have very similar intensity. [38] Accordingly, the two major bands of $H_5O_2^+$ in He droplets at 3600.4 cm^{-1} and 3678.6 cm^{-1} are assigned to the ν_s and ν_a stretch of the -OH_2 moieties in Zundel ion, respectively with a FWHM of 1.4 cm^{-1} and 2.7 cm^{-1}, respectively. The bands correspond to parallel and perpendicular transitions, respectively. While the ν_s appears as a single band, a shoulder is observed at the low frequency side of the ν_a band at ~ 3675 cm^{-1} and having intensity of ~ 20 % of the main peak. The small splitting of about 3 cm^{-1} may result from different effects, such as, interaction between the ν_a modes of the two H_2O moieties or from a slightly off-center position of the proton in $H_5O_2^+$. The splitting between the two asymmetric modes is estimated to be less than 1 cm^{-1}, whereas the bands should be degenerate under the effective D_{2d} symmetry.[38] The large difference in the intensity of the two components of the ν_a band is in disagreement with the results of calculations which predict very similar intensities.[38] The tunnel splitting associated with the hindered internal rotation of the water units in $H_5O_2^+$ may be another reason for the band splitting as was previously observed by Yeh *et. al.*[40] In this case, the intensity ratio of the sub-bands are determined by the population of the nuclear spin isomers, such as 1:3 for *para*:*ortho* modifications of water molecules. The tunnel splitting in the ground state of $H_5O_2^+$ was calculated to be ~ 1 cm^{-1}.[38, 40] Tunnel splitting due to internal rotation in dimers, such as $(HF)_2$ and $(H_2O)_2$ in He droplets have been previously documented.[41, 42] This splitting effect due to tunneling was also observed in the spectra of the He-H_2O^+ complexes.[30]

Figure 3 also shows the results of previous measurements of the $H_5O_2^+$ spectra for comparison. The band origins of free $H_5O_2^+$ ions are shown by green vertical bars at 3608.8 cm^{-1} and 3684.4 cm^{-1},[37] whose heights are proportional to the calculated infrared intensities.[38] The blue and black traces in Figure 3 are the results of measurements with He and Ar tagging, respectively.[10, 36] The two bands observed with He tagging are at ν_s = 3604.3 cm^{-1} and ν_a =3687.8 cm^{-1}, respectively.[10] It is seen that the ν_s and ν_a band positions of the $H_5O_2^+$ in helium droplets are redshifted by ~ 4 cm^{-1} (8 cm^{-1}) and ~ 9 cm^{-1} (6 cm^{-1}), respectively, as compared with those in the He tagged complexes (or free ions). The additional shift in He droplets with respect to He tagging is small and is just a few wavenumbers larger than the shifts typically observed for molecules in He droplets.[16, 18] The spectrum in He droplets also shows a factor of ~ 10 narrower bands as compared with He tagging, which may relate to lower temperature in He droplets as well as to homogeneous superfluid environment. Besides the shoulder of the ν_a band, the spectrum in He droplets shows no additional splitting of the bands, which suggests that the shared proton is symmetrically arranged with respect to the two water moieties. Such symmetry breaking phenomenon has previously been observed with Ar tagged (black) Zundel ion spectrum in Figure 3 which consists of four bands arising from the asymmetric and symmetric stretches of free (ν_a^{NB}, ν_s^{NB}) and Ar bound (ν_a^{Ar}, ν_s^{Ar}) H_2O units.[36]

We did not find any previous calculations for the He-$H_5O_2^+$ complexes. Calculations for Ar-$H_5O_2^+$ complexes yield the most favorable binding in the H-bound positions with Ar binding energy of D_e ~ 960 cm^{-1},[43] which is smaller than for the Ar-H_2O^+ of ~ 2500 cm^{-1}.[8] We assume that the binding energy of He atoms with $H_5O_2^+$ is also smaller than with H_2O^+, thus a smaller effect of the He environment on the spectra.

3.3. Formation of the Doped Ions and Laser Induced Release of Free Ions.

The results presented in this work show that the ionization of water doped He droplets leads to formation of diverse embedded ionic species, such as H_2O^+ and $H_5O_2^+$. The water cations may result from ionization of single water molecules, whereas the formation of Zundel cations must involve ionization of $(H_2O)_3$ or larger clusters, which are formed in the interior of the droplets upon pickup of several water molecules. It follows that He droplets provide a confining force strong enough to keep some of the ions formed upon EI from leaving the droplet, but weak enough for product of ion molecular reactions such as OH or possibly $OH\cdot(H_2O)_n$ to leave as it is evidenced

by the observation of the $H_5O_2^+$ spectrum in Figure 3. The ionization cross section of He atoms by 100 eV electrons is known to be 3.5×10^{-17} cm^2.[44] Using an estimated electron current flux of the order of 3×10^{-3} $A\cdot cm^{-2}$ and time of flight through the ion range of about 20 μs, the ionization efficiency per He atom is estimated to be about 10^{-5}. Therefore, about one in every 20 droplets is ionized. Although, a rather large mean free path of electrons in liquid helium of about 10 nm may facilitate the direct ionization of the dopants by electrons, it is more probable that electrons first produce He^+ ions or He* metastable atoms followed by the creation of ions via charge transfer or Penning ionization.[23] The ionization and ensuring ion-molecular reactions likely produces a large fraction of vibrationally excited ions, which cool down upon energy transfer to He droplets and concomitant evaporation of He atoms. For comparison, the release of 10000 cm^{-1} of energy will lead to evaporation of about 2000 He atoms. During this energy relaxation, some of the ions leave the droplet. Currently, the fraction of specific ionic products that remain inside the droplets is unknown; however, it is sufficiently large to obtain a high-quality infrared spectra.

In the initial study by Drabbels *et. al.*,[20] a close to linear dependence of the number of produced aniline ions from He droplets of about 2000 He atoms *vs* laser pulse energy was reported. It was hypothesized that non-thermal ejection of the ions upon IR excitation takes place.[20, 45] Later, studies[46] found a strongly nonlinear laser energy dependence of the ejection signal of protonated leu-enkephalin and its 18-crown-6 complex from He droplets of about 20000 atoms upon excitation by IR free electron laser with up to ~ 40 mJ per macro-pulse. The dominant yield of bare ions and small yield of He_n attached ions was argued to support the conjecture of the non-thermal ejection and is incompatible with the thermal evaporation mechanism.[20, 45, 46] Here, we show that the laser pulse energy dependence of the signal in Figure 2 (b) is in good agreement with the evaporation of all He atoms upon absorption of multiple infrared quanta.

Thermal evaporation of a droplet containing 7000 He atoms requires absorption of about 20 quanta of 3200 cm^{-1}. Multiple absorption during the ~ 7 ns laser pulse implies that the vibrationally excited ions relax to the ground state within the time faster than ~ 400 ps. This is about a factor of twenty faster than the relaxation time of the v_3 vibration of neutral water molecules in He droplets of ~ 7 ns as estimated from the laser saturation dependence of the depletion signal.[35] However, the values of this magnitude seem reasonable in view of the stronger interaction of the ions with He environment. Most likely the relaxation of the v_3 vibration into the ground state involves intermediate states, such as v_1, $2v_2$ and v_2. Previous spectroscopic studies

indicated fast vibrational relaxation of large amplitude bending and torsional modes with lifetime of ~ 1 ps.[16, 18] For comparison, the lower limit for lifetime in He-H_2O^+ complexes were estimated as $\tau_1 > 50$ ps and $\tau_3 > 150$ ps for the v_1 and v_3, bands, respectively.[30]

Here, we carry out model calculations for the efficiency of production of bare ions from He droplets, where the sizes follow a logarithm - normal distribution.[47] The calculations are performed at the maximum of the Lorentz line having FWHM, δv, with infrared intensity of *IRI*. We assumed Gaussian beam shape in the ion region of the QMS with the beam waist radius of w. For a droplet containing N atoms, we assume that the bare ion is produced upon absorption of k photons when $k \times \Delta N > N$. Here, $\Delta N = 3200\ \text{cm}^{-1}/H_{\text{evap}} \approx 400$, is the number of He atoms evaporated upon absorption of a single 3200 cm^{-1} quantum and H_{evap} (T = 2.7 K) = 7.8 cm^{-1} is the evaporation enthalpy for a single He atom.[48] The temperature of the droplet was estimated to be ~ 2.7 K considering that 7000 He atoms are evaporated during the 7 ns laser pulse and using saturated vapor pressure of He.[48] The probability for more than k photons being absorbed at a given laser flux is calculated using Poisson distribution.

Figure 4 shows the results of the model calculations. The ordinate in Figure 4 gives the efficiency of the ion production, A, which is expressed as an effective cross section area perpendicular to the droplet beam wherefrom the ions are completely extracted from the droplets. This efficiency is normalized on the area of the beam waist, πw^2. The abscissa shows the reduced laser flux, $F = E \cdot IRI/(\delta v \cdot \pi w^2)$, in which E is the laser pulse energy.

The results of droplets with average size of 7000 atoms are represented by the red curve in Figure 4. It is seen that the efficiency, A, is very small at small values of F after which it rises approximately linearly at $F > 2.5 \times 10^3$ mJ·km·mol^{-1}·cm^{-1}. Measurements in Figure 2 (b) show similar dependence with the efficiency taking off at $E > 1$ mJ. For the v_3 band of water ions $IRI \approx$ 500 km·mol^{-1}, [30] and $\delta v \approx 5$ cm^{-1}. The band appears narrower in Figure 2 (a) due to the non-linear laser pulse energy of the signal. The laser beam waist radius $w \approx 0.08$ cm is approximated from the nominal divergence of the laser beam of 4.5 mrad and 8.5 mrad in the horizontal and vertical directions, respectively, and the focal length of 25 cm. It follows that at E = 1 mJ, $F \approx$ 5000 mJ·km·mol^{-1}·cm^{-1}. Thus, the laser pulse energy in Figure 2 (b) at which the efficiency start rising seems to be a factor of ~ 2 larger than the calculated. The part of the discrepancy is due to the fact that the values of pulse energy in Fig. 2 (b) were measured at the entrance of the vacuum apparatus. The laser pulse energy in the ion range and the beam waist parameter were not measured in this

work due to lack of capability. In addition, the evaporation of ~ 100 last He atoms should likely be treated differently because they have larger values of H_{evap} due to their close proximity to the ions. The matrix shift of the transition will be smaller for an ion solvated by a small number of He atoms as compared to that in He droplets and the linewidth may be broadened due to higher temperature of the clusters, both leading to a smaller absorption cross section for infrared radiation. Note also that calculations in Figure 4 implied instant vibrational relaxation of cations in He droplets. In case of a finite, but currently unknown relaxation time, τ, the ions remain unavailable for re-excitation. This effect leads to higher laser flux required for the same effect. Considering these approximations, we conclude that the measured and calculated laser flux curves are in reasonable agreement. This agreement lends further support to the thermal evaporation mechanism of the He droplet upon laser excitation.

The nonlinear laser pulse energy dependence observed in this work and previously in Ref.[46] is inconvenient and may complicate the identification of the bands. Although in principle the intensities could be corrected using measured or calculated dependence of the signal on the laser pulse energy, this procedure may be unreliable for weak or congested bands. In particular, the weaker bands will appear even weaker and may escape the detection. The results in Figure 4 shows that the nonlinear effects are much smaller in small droplets containing 2000 atoms, whereas the initial dependence appears nearly linear in droplets containing average number of 800 He atoms. However, working with such small droplets is inconvenient, because of the droplet beam broadening upon pickup. The probability of an ion produced by EI to stay embedded likely decreases with the droplet size. In this work, droplets much smaller than ~ 7000 atoms could not be produced from our pulsed source, because of a rather abrupt jump in droplet sizes upon decrease of the nozzle temperature.[28, 29] Possible improvement of the technique may involve production of ions in larger droplets followed by subsequent moderation of the droplet size, which could be achieved upon multiple collisions with He atoms at room temperature.[49] Pertaining to ionic droplets, a better solution would be using an RF ion guide filled with He gas, as recently demonstrated by Scheier *et. al*.[50]

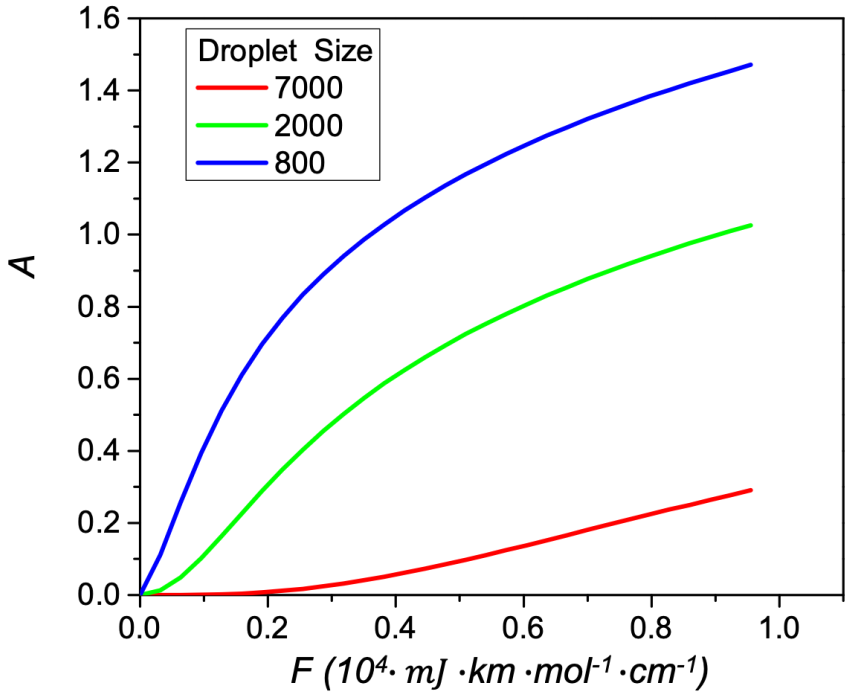

Figure 4. Efficiency of the ion production, *A*, vs reduced laser flux, *F*. See text for more details. Red, blue and green curves are for average droplet sizes of 7000, 2000 and 800 atoms, respectively.

4. Conclusions

Producing embedded ions by electron impact ionization of the doped droplets greatly increases the versatility of He droplet experiments. In fact, most of the contemporary He droplet spectrometers for neutral species involve mass spectrometers and can be upgraded to include ions. Large variety of the ions and ionic clusters could be formed starting with volatile molecular units, such as hydrocarbons, ammonia, or water molecules as done in this work. The OH-stretching spectra of H_2O^+ and $H_5O_2^+$ in helium droplets are of higher resolution as compared to the conventional tagging and matrix isolation methods. The ν_3 band of H_2O^+ has a matrix shift of about 26 cm^{-1} towards smaller energy. The spectra of larger ionic species, such as $H_5O_2^+$ are close to those of free species, consistent with weaker binding to the He environment. The obtained spectra are in agreement with the calculated structure of the free Zundel ion, where the proton is equidistant from the two water units. The non-linear power dependence of the spectral intensity on the laser pulse energy indicates that multiple photons are required to set the embedded ions free, which is broadly in agreement with the thermal evaporation of the entire droplet. The model calculations of the ion ejection efficiency as a function of laser flux show that for large droplet sizes, as in this work, a strong non-linear dependence is observed as compared to smaller droplet sizes, where the dependence is close to linear. Future experiments with small droplet sizes containing ~ 10^3 atoms may help in eliminating this non-linear effect.

5. Acknowledgements

This work was supported by the National Science Foundation under Grant CHE-1664990. The authors thank M. Johnson for making the data available to us for the spectra of Zundel ions tagged with Ar and He, which are presented in Figure 3.

6. References

1. Agmon, N.; Bakker, H. J.; Campen, R. K.; Henchman, R. H.; Pohl, P.; Roke, S.; Thämer, M.; Hassanali, A., Protons and Hydroxide Ions in Aqueous Systems. *Chemical Reviews* **2016,** *116*, 7642-7672.
2. Shuman, N. S.; Hunton, D. E.; Viggiano, A. A., Ambient and Modified Atmospheric Ion Chemistry: From Top to Bottom. *Chemical Reviews* **2015,** *115*, 4542-4570.
3. Tielens, A. G. G. M., *The Physics and Chemistry of the Interstellar Medium*. Cambridge University Press: Cambridge, 2005.
4. Begemann, M. H.; Gudeman, C. S.; Pfaff, J.; Saykally, R. J., Detection of the Hydronium Ion (H_3O^+) by High-Resolution Infrared-Spectroscopy. *Physical Review Letters* **1983,** *51*, 554-557.
5. Huet, T. R.; Pursell, C. J.; Ho, W. C.; Dinelli, B. M.; Oka, T., Infrared Spectroscopy and Equilibrium Structure of $H_2O^+(\tilde{X}\ ^2B_1)$. *The Journal of Chemical Physics* **1992,** *97*, 5977-5987.
6. Okumura, M.; Yeh, L. I.; Myers, J. D.; Lee, Y. T., Infrared-Spectra of the Solvated Hydronium Ion - Vibrational Predissociation Spectroscopy of Mass-Selected $H_3O^+.(H_2O)_n.(H_2)_m$. *Journal of Physical Chemistry* **1990,** *94*, 3416-3427.
7. Headrick, J. M.; Diken, E. G.; Walters, R. S.; Hammer, N. I.; Christie, R. A.; Cui, J.; Myshakin, E. M.; Duncan, M. A.; Johnson, M. A.; Jordan, K. D., Spectral Signatures of Hydrated Proton Vibrations in Water Clusters. *Science* **2005,** *308*, 1765-1769.
8. Dopfer, O., Microsolvation of the Water Cation in Argon: I. Ab Initio and Density Functional Calculations of $H_2O^+{-}Ar_n$ (n = 0–4). *The Journal of Physical Chemistry A* **2000,** *104*, 11693-11701.
9. Roithova, J.; Gray, A.; Andris, E.; Jasik, J.; Gerlich, D., Helium Tagging Infrared Photodissociation Spectroscopy of Reactive Ions. *Accounts of Chemical Research* **2016,** *49*, 223-230.
10. Johnson, C. J.; Wolk, A. B.; Fournier, J. A.; Sullivan, E. N.; Weddle, G. H.; Johnson, M. A., Communication: He-tagged Vibrational Spectra of the $SarGlyH^+$ and $H^+(H_2O)_{2,3}$ Ions: Quantifying Tag effects in Cryogenic Ion Vibrational Predissociation (CIVP) Spectroscopy. *Journal of Chemical Physics* **2014,** *140*, 221101.
11. Topfer, M.; Schmid, P. C.; Kohguchi, H.; Yamada, K. M. T.; Schlemmer, S.; Asvany, O., Infrared photodissociation of cold CH_3^+-He_2 complexes. *Molecular Physics* **2019,** *117*, 1481-1485.
12. Asvany, O.; Yamada, K. M. T.; Brunken, S.; Potapov, A.; Schlemmer, S., Experimental ground-state combination differences of CH_5^+. *Science* **2015,** *347*, 1346-1349.
13. Tsuge, M.; Tseng, C.-Y.; Lee, Y.-P., Spectroscopy of prospective interstellar ions and radicals isolated in para-hydrogen matrices. *Physical Chemistry Chemical Physics* **2018,** *20*, 5344-5358.
14. Jacox, M. E., The spectroscopy of molecular reaction intermediates trapped in the solid rare gases. *Chemical Society Reviews* **2002,** *31*, 108-115.
15. Tanyag, R. M. P.; Jones, C. F.; Bernando, C.; O'Connell, S. M. O.; Verma, D.; Vilesov, A. F., Experiments with large superfluid helium droplets. In *Cold chemistry: Molecular scattering and reactivity near absolute zero*, Dulieu, O.; Osterwalder, A., Eds. Royal Society of Chemistry: Cambridge, 2017; pp 401-455.

16. Toennies, J. P.; Vilesov, A. F., Superfluid Helium Droplets: A Uniquely Cold Nanomatrix for Molecules and Molecular Complexes. *Angewandte Chemie-International Edition* **2004,** *43*, 2622-2648.
17. Callegari, C.; Ernst, W. E., Helium Droplets as Nanocryostats for Molecular Spectroscopy - from the Vacuum Ultravoilet to the Microwave regime. In *Handbook of High-resolution Spectroscopy*, Quack, M.; Merkt, F., Eds. John Wiley & Sons, Ltd.: 2011; p 1551.
18. Choi, M. Y.; Douberly, G. E.; Falconer, T. M.; Lewis, W. K.; Lindsay, C. M.; Merritt, J. M.; Stiles, P. L.; Miller, R. E., Infrared Spectroscopy of Helium Nanodroplets: Novel Methods for Physics and Chemistry. *International Reviews in Physical Chemistry* **2006,** *25*, 15-75.
19. Verma, D.; Tanyag, R. M. P.; O'Connell, S. M. O.; Vilesov, A. F., Infrared Spectroscopy in Superfluid Helium Droplets. *Advances in Physics-X* **2018,** *4*, 1553569.
20. Smolarek, S.; Brauer, N. B.; Buma, W. J.; Drabbels, M., IR Spectroscopy of Molecular Ions by Nonthermal Ion Ejection from Helium Nanodroplets. *Journal of the American Chemical Society* **2010,** *132*, 14086-14091.
21. Bierau, F.; Kupser, P.; Meijer, G.; von Helden, G., Catching Proteins in Liquid Helium Droplets. *Physical Review Letters* **2010,** *105*, 133402.
22. Lewerenz, M.; Schilling, B.; Toennies, J. P., Successive capture and coagulation of atoms and molecules to small clusters in large liquid-helium clusters. *Journal of Chemical Physics* **1995,** *102*, 8191-8207.
23. Mauracher, A.; Echt, O.; Ellis, A. M.; Yang, S.; Bohme, D. K.; Postler, J.; Kaiser, A.; Denifl, S.; Scheier, P., Cold physics and chemistry: Collisions, ionization and reactions inside helium nanodroplets close to zero K. *Physics Reports-Review Section of Physics Letters* **2018,** *751*, 1-90.
24. Kuhn, M.; Renzler, M.; Postler, J.; Ralser, S.; Spieler, S.; Simpson, M.; Linnartz, H.; Tielens, A. G. G. M.; Cami, J.; Mauracher, A.; Wang, Y.; Alcami, M.; Martin, F.; Beyer, M. K.; Wester, R.; Lindinger, A.; Scheier, P., Atomically Resolved Phase Transition of Fullerene Cations Solvated in Helium Droplets. *Nature Communications* **2016,** *7*, 13550.
25. Davies, J. A.; Besley, N. A.; Yang, S. F.; Ellis, A. M., Probing Elusive Cations: Infrared Spectroscopy of Protonated Acetic Acid. *Journal of Physical Chemistry Letters* **2019,** *10*, 2108-2112.
26. Davies, J. A.; Besley, N. A.; Yang, S.; Ellis, A. M., Infrared spectroscopy of a small ion solvated by helium: OH stretching region of He_N–$HOCO^+$. *The Journal of Chemical Physics* **2019,** *151*, 194307.
27. Hartmann, M.; Miller, R. E.; Toennies, J. P.; Vilesov, A., Rotationally resolved spectroscopy of SF_6 in liquid-helium clusters - A molecular probe of cluster temperature. *Physical Review Letters* **1995,** *75*, 1566-1569.
28. Verma, D.; Vilesov, A. F., Pulsed Helium Droplet Beams. *Chemical Physics Letters* **2018,** *694*, 129-134.
29. Slipchenko, M. N.; Kuma, S.; Momose, T.; Vilesov, A. F., Intense Pulsed Helium Droplet Beams. *Review of Scientific Instruments* **2002,** *73*, 3600-3605.
30. Roth, D.; Dopfer, O.; Maier, J. P., Intermolecular Potential Energy Surface of the Proton-Bound H_2O^+– He dimer: Ab Initio Calculations and IR Spectra of the O–H Stretch Vibrations. *Physical Chemistry Chemical Physics* **2001,** *3*, 2400-2410.

31. Dopfer, O.; Roth, D.; Maier, J. P., Microsolvation of the Water Cation in Argon: II. Infrared Photodissociation Spectra of H_2O^+–Ar_n (n = 1−14). *The Journal of Physical Chemistry A* **2000,** *104*, 11702-11713.
32. Wagner, J. P.; McDonaldII, D. C.; Duncan, M. A., Near-infrared Spectroscopy and Anharmonic Theory of the $H_2O^+Ar_{1,2}$ Cation Complexes. *The Journal of Chemical Physics* **2017,** *147*, 104302.
33. Forney, D.; Jacox, M. E.; Thompson, W. E., The Vibrational Spectra of Molecular Ions Isolated in Solid Neon. X. H_2O^+, HDO^+, and D_2O^+. *The Journal of Chemical Physics* **1993,** *98*, 841-849.
34. Zhou, H.; Yang, R.; Jin, X.; Zhou, M., Infrared Spectra of the OH^+ and H_2O^+ Cations Solvated in Solid Argon. *The Journal of Physical Chemistry A* **2005,** *109*, 6003-6007.
35. Kuyanov, K. E.; Slipchenko, M. N.; Vilesov, A. F., Spectra of the ν_1 and ν_3 Bands of Water Molecules in Helium Droplets. *Chemical Physics Letters* **2006,** *427*, 5-9.
36. Hammer, N. I.; Diken, E. G.; Roscioli, J. R.; Johnson, M. A.; Myshakin, E. M.; Jordan, K. D.; McCoy, A. B.; Huang, X.; Bowman, J. M.; Carter, S., The Vibrational Predissociation Spectra of the $H_5O_2^+ \cdot RG_n$ (RG=Ar,Ne) Clusters: Correlation of the Solvent Perturbations in the Free OH and Shared Proton Transitions of the Zundel Ion. *Journal of Chemical Physics* **2005,** *122*, 244301.
37. Yeh, L. I.; Okumura, M.; Myers, J. D.; Price, J. M.; Lee, Y. T., Vibrational Spectroscopy of the Hydrated Hydronium Cluster Ions $H_3O^+.(H_2O)_n$ (n = 1, 2, 3). *Journal of Chemical Physics* **1989,** *91*, 7319-7330.
38. Vendrell, O.; Gatti, F.; Meyer, H.-D., Full Dimensional (15-dimensional) Quantum-Dynamical Simulation of the Protonated Water dimer. II. Infrared Spectrum and Vibrational Dynamics. *The Journal of Chemical Physics* **2007,** *127*, 184303.
39. Huang, X.; Braams, B. J.; Bowman, J. M., Ab Initio Potential Energy and Dipole Moment Surfaces for $H_5O_2^+$. *The Journal of Chemical Physics* **2005,** *122*, 044308.
40. Yeh, L. I.; Lee, Y. T.; Hougen, J. T., Vibration-Rotation Spectroscopy of the Hydrated Hydronium Ions $H_5O_2^+$ and $H_9O_4^+$. *Journal of Molecular Spectroscopy* **1994,** *164*, 473-488.
41. Kuyanov-Prozument, K.; Choi, M. Y.; Vilesov, A. F., Spectrum and Infrared Intensities of OH-stretching Bands of Water Dimers. *Journal of Chemical Physics* **2010,** *132*, 014304.
42. Douberly, G. E.; Miller, R. E., The Growth of HF Polymers in Helium Nanodroplets: Probing the Barriers to Ring Insertion. *Journal of Physical Chemistry B* **2003,** *107*, 4500-4507.
43. Douberly, G. E.; Walters, R. S.; Cui, J.; Jordan, K. D.; Duncan, M. A., Infrared Spectroscopy of Small Protonated Water Clusters, $H^+(H_2O)_n$ (n = 2−5): Isomers, Argon Tagging, and Deuteration. *The Journal of Physical Chemistry A* **2010,** *114*, 4570-4579.
44. Kim, Y.-K.; Rudd, M. E., Binary-encounter-dipole model for electron-impact ionization. *Physical Review A* **1994,** *50*, 3954-3967.
45. Zhang, X. H.; Brauer, N. B.; Berden, G.; Rijs, A. M.; Drabbels, M., Mid-infrared spectroscopy of molecular ions in helium nanodroplets. *Journal of Chemical Physics* **2012,** *136*, 044305.
46. González Flórez, A. I.; Ahn, D. S.; Gewinner, S.; Schollkopf, W.; von Helden, G., IR Spectroscopy of Protonated Leu-enkephalin and its 18-crown-6 Complex Embedded in Helium Droplets. *Physical Chemistry Chemical Physics* **2015,** *17*, 21902-21911.
47. Lewerenz, M.; Schilling, B.; Toennies, J. P., A new scattering deflection method for determining and selecting the sizes of large liquid clusters of ^{4}He. *Chemical Physics Letters* **1993,** *206*, 381-387.

48. Donnelly, R. J.; Barenghi, C. F., The observed properties of liquid helium at the saturated vapor pressure. *Journal of Physical and Chemical Reference Data* **1998,** *27*, 1217-1274.
49. Gomez, L. F.; Loginov, E.; Sliter, R.; Vilesov, A. F., Sizes of large He droplets. *Journal of Chemical Physics* **2011,** *135*, 154201.
50. Tiefenthaler, L.; Ameixa, J.; Martini, P.; Albertini, S.; Ballauf, L.; Zankl, M.; Goulart, M.; Laimer, F.; Haeften, K. v.; Zappa, F.; Scheier, P., An intense source for cold cluster ions of a specific composition. *Review of Scientific Instruments* **2020,** *91*, 033315.